PHYSICAL REVIEW D **82,** 045019 (2010)

How to run through walls: Dynamics of bubble and soliton collisions

John T. Giblin, Jr.,[1,2,*] Lam Hui,[3,4,5,†] Eugene A. Lim,[3,‡] and I-Sheng Yang[3,§]

[1]*Department of Physics, Kenyon College, Gambier, Ohio 43022, USA*
[2]*Perimeter Institute for Theoretical Physics, 31 Caroline Street N, Waterloo, Ontario N2L 2Y5, Canada*
[3]*ISCAP and Department of Physics, Columbia University, New York, New York 10027, USA*
[4]*Institute for Advanced Study, Princeton, New Jersey 08540, USA*
[5]*CCPP and Department of Physics, New York University, New York, New York 10003, USA*

(Received 7 June 2010; published 17 August 2010)

It has recently been shown in high resolution numerical simulations that relativistic collisions of bubbles in the context of a multivacua potential may lead to the creation of bubbles in a new vacuum. In this paper, we show that scalar fields with only potential interactions behave like free fields during high-speed collisions; the kick received by them in a collision can be deduced simply by a linear superposition of the bubble wall profiles. This process is equivalent to the scattering of solitons in $1 + 1$ dimensions. We deduce an expression for the field excursion (shortly after a collision), which is related simply to the field difference between the parent and bubble vacua, i.e. contrary to expectations, the excursion cannot be made arbitrarily large by raising the collision energy. There is however a minimum energy threshold for this excursion to be realized. We verify these predictions using a number of $3 + 1$ and $1 + 1$ numerical simulations. A rich phenomenology follows from these collision-induced excursions—they provide a new mechanism for scanning the landscape, they might end/begin inflation, and they might constitute our very own big bang, leaving behind a potentially observable anisotropy.

DOI: 10.1103/PhysRevD.82.045019 PACS numbers: 11.27.+d

I. INTRODUCTION

The recent interest in the phenomenology of the string landscape [1] has sparked a resurgence of interests in the physics of bubbles and bubble collisions. An understanding of such collisions promises much: a prediction of observational consequences of such collisions [2–8], an insight into the interaction of nonperturbative objects such as domain walls in general, a more complete treatment of the bubble counting measure [9,10], possibly a new method of scanning the landscape, and many other wonderful things. As Coleman [11] succinctly asked in his seminal paper on the fate of the false vacuum "…bubble walls begin to collide. What happens then? Can such events be accommodated in the history of the early universe?"

The *kinematics* of wall collisions is well understood: provided one knows the nature of the incoming and outgoing walls (if indeed walls are the only by-products), the wall trajectories can be obtained by energy-momentum conservation [12–15]. Our goal, on the other hand, is to understand the collision *dynamics* [16]: how does the field configuration evolve through a collision?

One fruitful approach to understanding the nonperturbative physics involved is numerical, namely, lattice simulations of bubble wall collisions. This was pioneered almost 30 years ago by Hawking, Moss, and Stewart [17]. Despite their relatively (by today's computational standards) low resolution,[1] their $1 + 1$ dimensional simulations discovered an interesting result that was not predicted by analytic methods: the collision of two true vacuum bubbles creates a relatively long live pocket of false vacuum which eventually collapse under differential pressure between the spacetime regions. This result was not well understood or exploited until recently. In high resolution, $3 + 1$ dimensional, numerical simulations, it was shown that not only is this formation of false vacuum pocket a fairly robust effect, the right kind of potential can produce a new, stable bubble of a different vacuum ([20], henceforth EGHL). Furthermore, such *classical transitions* can be quite elastic—coherent bubble walls form immediately after collisions with little dissipative losses in the form of scalar radiation. EGHL also showed that whether such transition occurs is dependent on both the energy of the collision, and the height of the potential barrier between the progenitor bubble vacuum and the progeny bubble vacuum. The setup is illustrated in Fig. 1.

In this paper, we wish to extend the work of EGHL, beginning with the question: what determines the size of the collision-induced excursion? By this we mean the field excursion at $x = 0$ (the location of the collision), from immediately before to immediately after the collision

*giblinj@kenyon.edu
†lhui@astro.columbia.edu
‡eugene.a.lim@gmail.com
§isheng.yang@gmail.com

[1]See also [18,19], where lattice simulations were used to investigate the collisions of subhorizon bubbles during a first order electroweak phase transition.

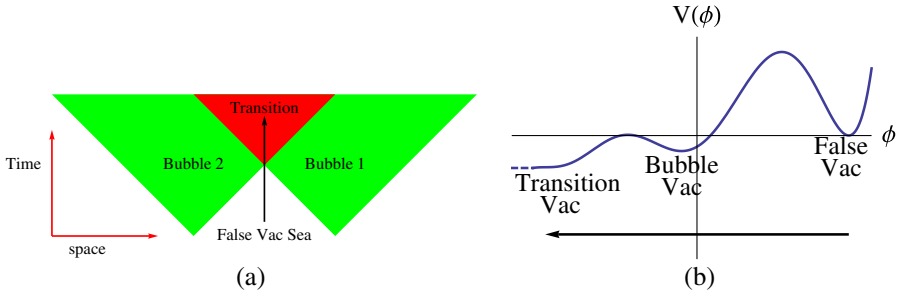

FIG. 1 (color online). (a) A spacetime diagram showing the collision of two bubbles embedded in a false vacuum sea, in a frame in which the two bubbles nucleate at the same time. We refer to the overlap between the bubbles as the transition region—here, the scalar field is generally kicked by the collision to somewhere else in field space. (b) A schematic diagram showing the potential for the scalar field. The arrow denotes the scalar field kick as seen by an observer following the black arrow in (a). This is the kick immediately after a collision, which is realized as long as a certain minimum condition is met. Where the field will roll to in the long run depends on the precise layout of the landscape in the transition region. Note that only one bubble vacuum is shown. The other bubble might inhabit the same or some other vacuum. Note also the field space does not have to be one dimensional.

(Fig. 1). Naively, one might think that the excursion depends on the collision energy—the higher the energy, the farther the scalar field could go—as if the kinetic energy stored in the bubble walls can be tapped to initiate motions in field space. This kind of reasoning proves to be misleading, however.

Let us try to gain some insight by simplifying the problem. Two colliding bubbles have $SO(2,1)$ symmetry realized in spacelike H_2 surfaces. As the bubble walls accelerate and the bubbles grow in size, H_2 becomes almost planar and the walls are boosted to be very thin.[2] A high-speed collision is a $1+1$ dimensional problem between two planar walls, equivalent to the collision of two kink solitons. Much is known about the scattering of solitons in for instance the famous sine-Gordon model (the Appendix). We will be able to deduce some general model independent results in the relativistic collision limit, including the case of multiple scalar fields. And we will find that the collision-induced field excursion is in fact bounded, and given by a simple expression involving the field difference between the false and the bubble vacua (Sec. II). There is a minimum energy threshold that must be reached for this maximal field excursion to be realized, which is derived in Sec. III. These analytic predictions are verified with numerical experiments in Sec. IV. We will digress a bit in Sec. V to consider cases where the excursion takes the field through multiple local minima.

These collision-induced field excursions open up a rich set of questions, including: How do they impact inflation? What are the observational signatures if we reside in the transition region (Fig. 1)? What happens when there are multiple collisions? We will explore these questions in Sec. VI. For the most part, we focus in this paper on scalar field models with canonical kinetic terms and potential interactions, and work in flat space. Relaxing these assumptions will be discussed in Sec. VI as well.

[2]Note that this has nothing to do with the "thin wall condition" of the instanton. Regardless of how the bubbles were nucleated, in the collision frame the walls are naturally boosted and thin.

II. THE FREE-PASSAGE APPROXIMATION—IMPLICATION FOR THE COLLISION-INDUCED FIELD EXCURSION

We are interested in solutions to the scalar field equation,

$$\Box\phi = \frac{\partial V}{\partial \phi}, \tag{1}$$

which contain bubble/domain wall configurations. Here, $V(\phi)$ is a potential with two or more metastable minima. In particular, we are interested in how the domain/bubble walls interact in a collision. It should be emphasized that while we are primarily motivated by cosmological applications, much of our discussion carries over to the collision of domain or solitonic walls in broader contexts.

For the moment, we focus on a single scalar field ϕ. The generalization to multiple fields will be discussed below. We work in Minkowski space and defer a discussion of gravity to Sec. VI. Some of our numerical simulations do have an expanding background, but the backreaction of the scalar field on the geometry is not properly taken into account.

Let us follow the strategy laid out in Sec. I, and take the high-speed/large bubble limit, in which case the collision problem becomes effectively $1+1$ dimensional:

$$-\partial_t^2\phi + \partial_x^2\phi = \frac{\partial V}{\partial \phi}, \tag{2}$$

where t is time and x labels the axis of collision.

We are interested in a potential of the sort schematically shown in Fig. 2(a). The "false" (or parent) vacuum is denoted by ϕ^A, and the two bubble vacua are ϕ^B and $\phi^{B'}$, respectively. In other words, the collision of interest

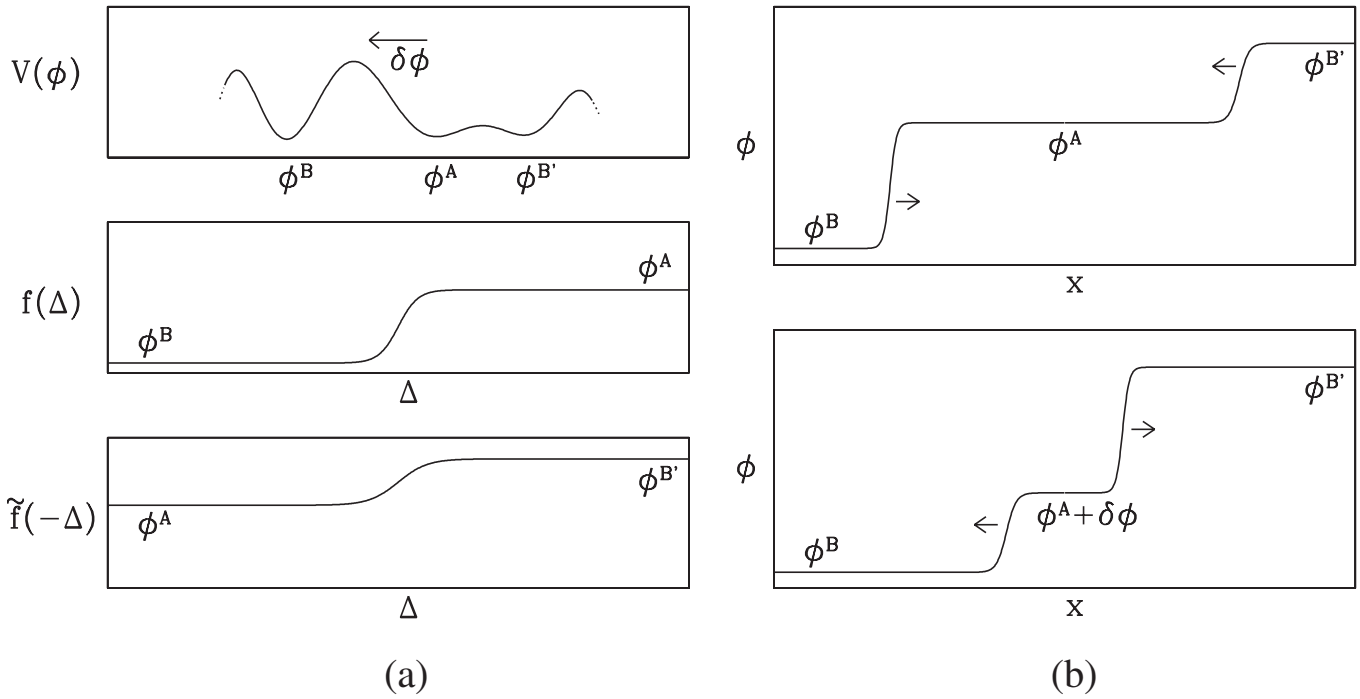

FIG. 2. (a) The top panel displays part of a landscape of local minima of the potential V of some scalar field ϕ. $\delta\phi$ is the kick induced by collision. The middle panel shows the solitonic profile that interpolates between ϕ^B and ϕ^A. The bottom panel shows the solitonic profile that interpolates between $\phi^{B'}$ and ϕ^A. (b) The top panel depicts the scalar field ϕ as a function of position x at some time $t < 0$ in the far past, before the two solitons collide. These two solitons can be thought of as part of bubble walls: the bubble on the left has an interior scalar field value of ϕ^B; the bubble on the right has an interior scalar value of $\phi^{B'}$; ϕ^A in between is the false/parent vacuum. The bottom panel shows the scalar profile soon after the solitons collide. What is assumed is the free passage of waveforms [Eq. (5)]: the top panel comes from summing f to the left of $\tilde{f}$, the bottom from summing f to the right of $\tilde{f}$. Note how the field value in the collision region shifts from ϕ^A precollision to $\phi^A + \delta\phi$ postcollision, with $\delta\phi = \phi^B + \phi^{B'} - 2\phi^A$. In other words, the outgoing objects are *different* from the incoming solitons: they interpolate between different field values.

is between two walls, one spanning from ϕ^A to ϕ^B, and the other from ϕ^A to $\phi^{B'}$. We will treat these vacua as roughly degenerate, so that the wall speed is nearly constant. This conflicts somewhat with our picture of generally accelerating bubble walls, but the degeneracy assumption is not really crucial—much of our discussion carries over to the nondegenerate case with the speed u below taken to be the wall velocity just prior to collision.

In the rest frame of the respective solitonic walls, the wall profiles are denoted by f and $\tilde{f}$ [Fig. 2(a)], i.e. they satisfy the equations:

$$\frac{d^2 f(\Delta)}{d\Delta^2} = \frac{\partial V(f)}{\partial f}, \qquad \frac{d^2 \tilde{f}(\Delta)}{d\Delta^2} = \frac{\partial V(\tilde{f})}{\partial \tilde{f}}, \tag{3}$$

with the respective boundary conditions $f(\Delta \to \infty) = \phi^A$, $f(\Delta \to -\infty) = \phi^B$, and $\tilde{f}(\Delta \to \infty) = \phi^A$, $\tilde{f}(\Delta \to -\infty) = \phi^{B'}$.

Boosting to a frame in which the two solitons collide at equal and opposite speed u, the wall profiles as a function of space and time are

$$f\left(\frac{x - ut}{\sqrt{1-u^2}}\right), \qquad \tilde{f}\left(-\frac{x + ut}{\sqrt{1-u^2}}\right). \tag{4}$$

Here, f represents the right-going soliton and $\tilde{f}$ represents the left-going one. When the solitons are far apart, say at $t \to -\infty$, the solitons only interact very weakly with each other, and hence we can represent the *total* scalar field solution ϕ as a linear superposition of the two solutions f and $\tilde{f}$

$$\phi(t, x) = f\left(\frac{x - ut}{\sqrt{1-u^2}}\right) + \tilde{f}\left(-\frac{x + ut}{\sqrt{1-u^2}}\right) - \phi^A. \tag{5}$$

The constant shift of $-\phi^A$ is necessary so that at $t < 0$ (prior to collision), the scalar field ϕ takes the (false/parent vacuum) value ϕ^A between the two walls, and the fields to the far left and far right take the values ϕ^B and $\phi^{B'}$, respectively [upper panel of Fig. 2(b)].

While it is easy to see that Eq. (5) is a good approximation when the two solitons are far apart, the key insight in understanding soliton collisions is that Eq. (5) remains a good approximation even during and slightly past the collision time $t = 0$, for sufficiently energetic collisions i.e. $u \to 1$. In this limit, both the spatial and time gradient

terms dominate over the potential term in Eq. (2) at the walls (the wall profiles effectively become step functions):

$$|\partial_x^2\phi|, \qquad |\partial_t^2\phi| \gg |\frac{\partial V}{\partial\phi}|, \qquad -\partial_t^2\phi + \partial_x^2\phi \sim 0. \quad (6)$$

Meanwhile, away from the walls, the scalar field sits roughly at the corresponding local minimum where the derivative of the potential is also small.

A superposition of the two waveforms f and $\tilde{f}$ as in Eq. (5) should therefore be a good solution to the linear wave Eq. (6), as long as $u \sim 1$. This should hold even postcollision. [Let us postpone for the moment a discussion of when this approximation Eq. (5) ceases to be accurate.] Taking this seriously gives a very interesting prediction: around $x = 0$ where the collision happens, $\phi = \phi^A$ before collision, whereas $\phi = \phi^B + \phi^{B'} - \phi^A$ after collision. In other words, compare the upper and lower panels of Fig. 2(b): the precollision configuration is obtained by superimposing f to the left of $\tilde{f}$, whereas the postcollision configuration comes from superimposing f to the right of $\tilde{f}$ [taking care to include the constant shift $-\phi^A$ as in Eq. (5)]. In other words, the two wall profiles (or waveforms) *freely pass through* each other, creating a region where the scalar field takes a value that is neither the original parent vacuum value ϕ^A, nor the bubble interior values ϕ^B or $\phi^{B'}$. We say that the collision produces a *kick* to the scalar field of

$$\delta\phi = \phi^B + \phi^{B'} - 2\phi^A. \quad (7)$$

This is illustrated in Fig. 2(b). We refer to this observation as the *free-passage approximation*.

It is worth noting that even as the two profiles or waveforms f and $\tilde{f}$ freely pass through each other, the nature of the solitons has actually changed: while the incoming solitons interpolate between ϕ^A and ϕ^B (and between ϕ^A and $\phi^{B'}$), the outgoing objects interpolate between $\phi^A + \delta\phi$ and ϕ^B (and between $\phi^A + \delta\phi$ and $\phi^{B'}$). Indeed, the outgoing objects strictly speaking are not even solitons, since $\phi^A + \delta\phi$ is not in general a stationary point of the potential [see Fig. 2(a)]. One could think of the collision process as a scattering event. The free passage of waveforms is reminiscent of the impulse approximation used in high energy scattering.

The free-passage approximation should break down soon after free passage itself. As illustrated in the lower panel of Fig. 2(b), there is a region between the outgoing objects where the field gradient is small while the derivative of the potential is non-negligible (i.e. $\phi^A + \delta\phi$ is not a stationary point of the potential). Equation (6) therefore ceases to be a good approximation, and one must account for the effect of the potential.

Under what condition then, is the free-passage kick $\delta\phi = \phi^B + \phi^{B'} - 2\phi^A$ actually realized? In the subsequent sections, we will estimate, and verify with numerical calculations, a minimum collision energy/velocity in order for the free-passage kick to be successfully executed. If the collision is not sufficiently energetic, the scalar field can still make a fleeting excursion of a similar size, but it quickly retreats back to the false or bubble vacua thereafter. We will refer to this as an unsuccessful or failed kick. Anticipating a bit numerical experiments we will run, the distinction between a successful and a failed kick is illustrated in Figs. 6 and 7.

It is important to emphasize that our primary goal here is to work out the field excursion shortly after a collision, rather than its long term behavior. As noted above, the free-passage approximation generally breaks down soon after a collision (even if the kick is successful), and therefore cannot be used to predict the long term outcome of the field dynamics. The short term outcome, however, does have long term implications: if the free-passage kick fails, the field ϕ would inevitably roll back to the false or bubble vacua; if the free-passage kick succeeds, the field's long term evolution would be driven by whatever basin of attraction it happens to be in after the kick. If $\phi^A + \delta\phi$ is in the basin of attraction of some new vacuum, then we can have the formation of a new vacuum bubble.

This is why the case illustrated in Fig. 2 is in a sense not so interesting, for no matter whether in the short term the free-passage kick succeeds or not, in the long run it would not roll to any new vacuum. A more interesting example is one where $\phi^B = \phi^{B'}$ i.e. colliding two bubbles inhabiting the same vacuum. This is illustrated in Fig. 3.

What happens in this case is that the collision-induced kick $\delta\phi = 2(\phi^B - \phi^A)$ could lead to the formation of a new bubble that is at neither the parent vacuum ϕ^A nor the bubble vacuum ϕ^B. Indeed, in the example depicted in Fig. 3, $\delta\phi$ is sufficiently large that the kick takes the field over a new barrier (at the far left). Provided the collision satisfies a minimum energy condition to be derived in the next section, we would have an interesting outcome: the creation of a bubble of a new vacuum in the collision region.

It is worth noting that the free-passage approximation predicts the walls retain their integrity through a collision (even as they change character: a wall that interpolates between ϕ^B and ϕ^A become one that interpolates between ϕ^B and $\phi^A + \delta\phi$). It is perhaps surprising that the collision does not result primarily in dissipation into scalar radiation instead. The reason is because at a high collision speed, the (potential) interactions are negligible and the field is essentially free [Eq. (6)]. As we will see in Sec. IV, this simple reasoning appears to be borne out by numerical simulations. There will be some radiative loss, but the amount tends to be small. The potential interactions are of course important after the free-passage kick. For instance, in the example depicted in Fig. 3, after a successful kick, the scalar field will roll toward whatever new vacuum exists on the far left. The outgoing walls will adjust their

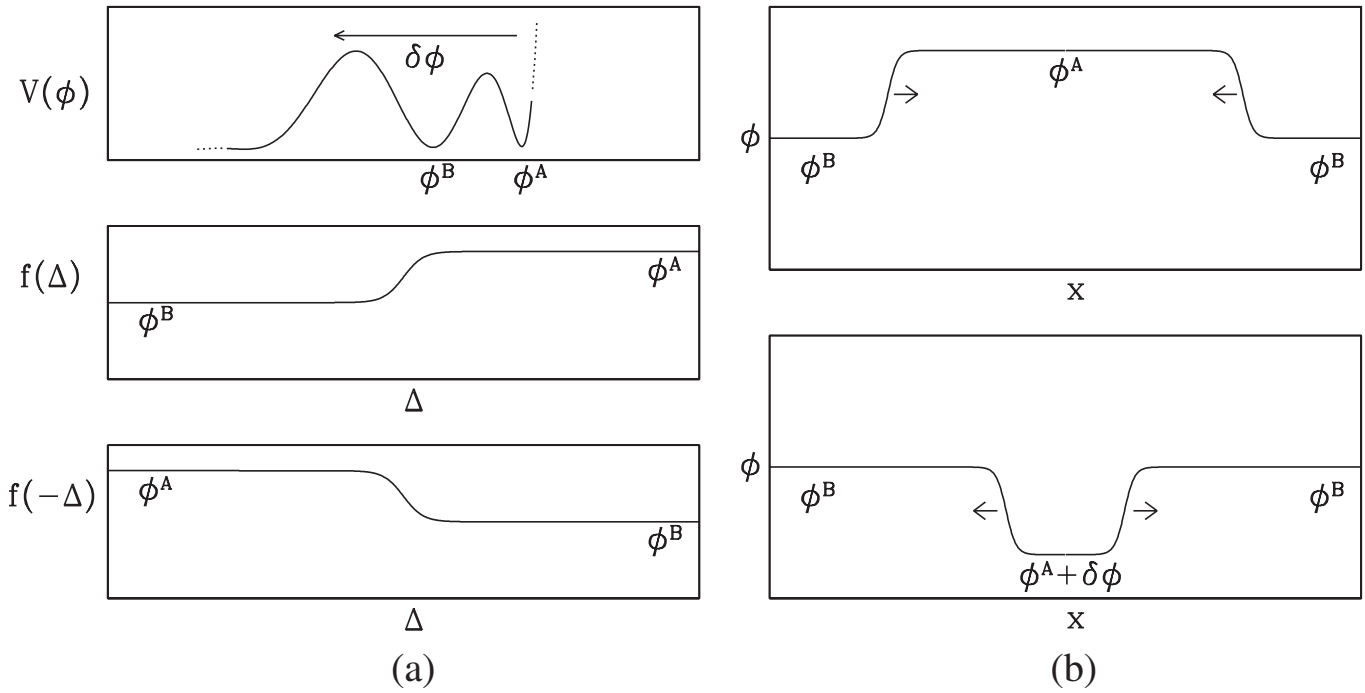

FIG. 3. Analog of Fig. 2 for $\phi^{B'} = \phi^B$, such that the kick $\delta\phi = 2(\phi^B - \phi^A)$. As before, the incoming configuration in the top panel of (b) corresponds to summing $f(\Delta)$ to the left of $f(-\Delta)$, while the outgoing configuration in the bottom panel of (b) corresponds to summing $f(\Delta)$ to the right of $f(-\Delta)$ [more precisely: the free-passage solution in Eq. (5)]. Physically, one can think of this as the annihilation of a soliton and an antisoliton giving rise to a *different* pair of objects. From the point of view of bubble collisions, we have here two ϕ^B bubbles (immersed in the parent vacuum sea ϕ^A) colliding with each other, triggering a new bubble forming at $\phi^A + \delta\phi$ (at least momentarily).

profiles, as the region between them relaxes toward this new vacuum.

Conversely, if the collision does not satisfy the minimum energy condition, then the field excursion barely reaches $\delta\phi = 2(\phi^B - \phi^A)$, and eventually retreats back to the false/parent or bubble vacua, ϕ^A or ϕ^B. As we will see, this can happen even if, *momentarily*, the field has crossed the new potential barrier to the left. The retreat is due to tendency of the spatial gradient force to counteract the (free passage implied) field excursion. In the language of solitons, a retreat (i.e. an unsuccessful kick) means the outgoing pair of (solitonlike) objects cannot overcome their mutual attraction, a phenomenon we will observe in numerical simulations (Fig. 7).

Lastly, to cover the range of possible outcomes, consider a situation where contrary to Fig. 3, the kick $\delta\phi = 2(\phi^B - \phi^A)$ is not large enough to take the scalar field over the new barrier to the left. In this case, even if the kick were successful, the scalar field would have to roll back to ϕ^B or even ϕ^A eventually. More quantitatively, one can see that at the collision point ($x = 0$),

$$\frac{\partial^2\phi}{\partial t^2} = \frac{\partial^2\phi}{\partial x^2} - \frac{\partial V}{\partial\phi} > 0 \tag{8}$$

after free passage (recalling that the free-passage approximation predicts vanishing space and time derivatives at $x = 0$ after a collision). Therefore, the field retreats back toward ϕ^B or ϕ^A.

In summary, the free-passage kick of $\delta\phi = \phi^B + \phi^{B'} - 2\phi^A$, or $\delta\phi = 2(\phi^B - \phi^A)$ if the bubbles inhabit the same vacuum, constitutes a maximal field excursion shortly after a collision.

Generalization to multiple fields.—Let us conclude this section by pointing out that all of our arguments above translate in a straightforward manner to the case of multiple scalar fields, i.e. the equation of motion is

$$\Box\vec{\phi} = \frac{\partial V}{\partial\vec{\phi}}. \tag{9}$$

Suppose we have a landscape of a multiple-dimensional scalar $\vec{\phi}$. Suppose further that we have a parent or false vacuum sea at $\vec{\phi}^A$, within which there are two bubbles, one at $\vec{\phi}^B$ and one at $\vec{\phi}^{B'}$. When these two bubbles collide, the free-passage approximation tells us that the scalar field should receive a kick in the collision region from $\vec{\phi}^A$ to $\vec{\phi}^A + \delta\vec{\phi}$, where

$$\delta\vec{\phi} = \vec{\phi}^B + \vec{\phi}^{B'} - 2\vec{\phi}^A. \tag{10}$$

The situation is illustrated in Fig. 4. This prediction for $\delta\vec{\phi}$ should be accurate momentarily after a high-speed collision. Note that the linear superposition [Eq. (5)] actually

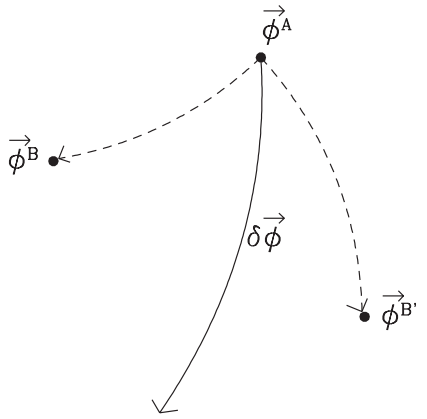

FIG. 4. A schematic diagram *in field space*, illustrating the collision-induced kick in a landscape of a multidimensional scalar field $\vec{\phi}$. $\vec{\phi}^A$ denotes the false/parent vacuum value. Embedded inside the false vacuum sea are two bubbles, one inhabiting the local minimum at $\vec{\phi}^B$, the other at $\vec{\phi}^{B'}$. When these two bubbles collide, the field in the collision region would undergo an excursion $\delta\vec{\phi}$ (at least momentarily) away from $\vec{\phi}^A$, where $\delta\vec{\phi}$ is simply the vector sum of $\vec{\phi}^B - \vec{\phi}^A$ and $\vec{\phi}^{B'} - \vec{\phi}^A$. The dashed lines denote the bubble wall profile from vacuum A to vacuum B and vacuum B', respectively. The solid line is a linear superposition of these two wall profiles, and illustrates the field excursion upon bubble collision predicted by free passage [Eq. (19)].

says more than this: not only is there a vector sum rule governing the end point of the excursion Eq. (10), the colliding wall profiles, which are not necessarily straight lines in field space, also add to give the excursion profile.

Let us close by noting two crucial assumptions: that there are only potential interactions, and that the multi-scalar kinetic term (in the action) is diagonalized and canonical. We will discuss deviations from these in Sec. VI.

III. A MINIMUM ENERGY CONDITION FOR A SUCCESSFUL KICK

Let us consider under what condition the free-passage approximation is accurate, i.e. that the scalar field successfully realizes the field excursion $\delta\phi = 2(\phi^B - \phi^A)$ in the example depicted in Fig. 3. More general situations, such as that depicted in Fig. 4, will be considered later.

The field configuration can be expressed as

$$\phi(t, x) = \phi_{\rm fp}(t, x) + \sigma(t, x), \tag{11}$$

where $\phi_{\rm fp}$ is the free passage solution which is a linear superposition of right-going soliton and left-going antisoliton Eq. (5):

$$\phi_{\rm fp}(t, x) = f\left(\frac{x - ut}{\sqrt{1 - u^2}}\right) + f\left(-\frac{x + ut}{\sqrt{1 - u^2}}\right) - \phi^A \tag{12}$$

and σ represents the deviation from the actual solution from the free-passage solution. The free-passage approximation is accurate only when σ is small compared to, say, the free-passage kick itself i.e. $\sigma/\delta\phi \ll 1$. We will use the shorthand $f_R \equiv f([x - ut]/\sqrt{1 - u^2})$ and $f_L \equiv f(-[x + ut]/\sqrt{1 - u^2})$.

Using Eq. (3), we can rewrite the ϕ equation of motion as an equation for σ

$$\Box\sigma = \left.\frac{\partial V}{\partial\phi}\right|_{\phi=\phi_{\rm fp}+\sigma} - \left.\frac{\partial V}{\partial\phi}\right|_{\phi=f_R} - \left.\frac{\partial V}{\partial\phi}\right|_{\phi=f_L}. \tag{13}$$

The question is under what condition does σ remain small after the right-going soliton and left-going antisoliton have passed through each other?

A formal solution to Eq. (13) is

$$\sigma(t, x) = -\int_{-\infty}^{t} dt' \int_{x-(t-t')}^{x+t-t'} dx' g(t', x') \tag{14}$$

with the kernel function $g(t', x')$

$$g \equiv \left.\frac{\partial V}{\partial\phi}\right|_{\phi=\phi_{\rm fp}+\sigma} - \left.\frac{\partial V}{\partial\phi}\right|_{\phi=f_R} - \left.\frac{\partial V}{\partial\phi}\right|_{\phi=f_L}. \tag{15}$$

We estimate this integral by ignoring σ in the integrand (first term in g)—the free passage approximation is self-consistent if the resulting estimate for σ is indeed small. We are most interested in its value at $x = 0$, and by making a change of variables $X' \equiv x'/\sqrt{1 - u^2}$ and $T' \equiv ut'/\sqrt{1 - u^2}$ we can rewrite it as follows to show its explicit dependence on the velocity u:

$$\sigma(t, 0) = -\frac{1 - u^2}{u} \int_{-\infty}^{ut/\sqrt{1-u^2}} dT' \int_{-(t-t')/\sqrt{1-u^2}}^{t-t'/\sqrt{1-u^2}} dX' \times \left[\left.\frac{\partial V}{\partial\phi}\right|_{\phi=f_R+f_L-\phi^A} - \left.\frac{\partial V}{\partial\phi}\right|_{\phi=f_R} - \left.\frac{\partial V}{\partial\phi}\right|_{\phi=f_L}\right]. \tag{16}$$

Note that as $u \to 1$, $\sigma \to 0$ confirming our assertion that free passage is the right approximation in the relativistic limit. The time t we are interested in is when the solitons have just passed through each other, i.e. $ut/\sqrt{1 - u^2} = \mu^{-1}$, where μ^{-1} is the rest-frame thickness of the bubble walls. The thickness can be estimated by $\mu^2 \sim |\partial^2 V/\partial\phi^2|$ evaluated at the barrier that separates the parent and the bubble vacua. The integrand in Eq. (16) vanishes when the two incoming solitons are far apart, and is dominated by when $T' \sim \pm\mu^{-1}$. A reasonable estimate can be obtained by focusing on what happens postcollision, when the integrand is dominated by the first term $\partial V/\partial\phi$ at $\phi = 2\phi^B - \phi^A$. Therefore, we have

$$\sigma \sim -\frac{1 - u^2}{u^2}\frac{1}{\mu^2}\left.\frac{\partial V}{\partial\phi}\right|_{\phi=2\phi^B-\phi^A}. \tag{17}$$

As we argued above, self-consistency of the free-passage

approximation demands that $|\sigma| \ll |\delta\phi| = |2(\phi^B - \phi^A)|$. To be concrete, we demand that for the field to continue marching onward after the free passage kick, the collision velocity must satisfy

$$\gamma^2 = \frac{1}{1-u^2} \gtrsim 1 + \frac{\alpha^{-1}}{|\phi^B - \phi^A|} \frac{1}{\mu^2} \left| \frac{\partial V}{\partial \phi} \right|_{\phi = 2\phi^B - \phi^A}, \tag{18}$$

where the efficiency factor $\alpha^{-1} \approx 5.5$ is determined numerically. This efficiency factor tells us how much smaller $|\sigma|$ has to be compared to $|\delta\phi|$ for free passage to be a good approximation.

A collision that satisfies the condition Eq. (18) can successfully realize the free-passage kick. This does not by itself mean there is a transition to a new vacuum—for that to happen, the kick must take the field to within the basin of attraction of a new vacuum. Conversely, collisions that do not satisfy Eq. (18) produce a fleeting field excursion that barely makes $\delta\phi = 2(\phi^B - \phi^A)$, and the field beats a retreat soon after.

There exists an important caveat to Eq. (18): if $\partial V/\partial\phi$ at $\phi = 2\phi^B - \phi^A$ vanishes, this minimum energy condition must be reevaluated. What we have done in writing down Eq. (18) [and Eq. (17)] was to approximate the full integrand in Eq. (16) by one single term. This is obviously a simplification that needs to be fixed if the term we have chosen happens to vanish. This happens, for instance, when $\phi = 2\phi^B - \phi^A$ is another local minimum of the potential.[3]

Finally, an intriguing counter example to the above caveat is the well-known sine-Gordon soliton, where the free-passage field excursion is successfully realized no matter what value $u > 0$ takes [21]. In this case, the condition Eq. (18) is both trivial and exact. A brief summary is provided in the Appendix.

Generalization to multiple fields.—The above reasoning translates straightforwardly to the case of multiple scalar fields, with the equation of motion (9). The solution can be expressed as $\vec{\phi} = \vec{\phi}_{\rm fp} + \vec{\sigma}$, with the free-passage solution:

$$\vec{\phi}_{\rm fp}(t,x) = \vec{f}\left(\frac{x-ut}{\sqrt{1-u^2}}\right) + \vec{\tilde{f}}\left(-\frac{x+ut}{\sqrt{1-u^2}}\right) - \vec{\phi}^A, \tag{19}$$

where $\vec{f}$ interpolates between $\vec{\phi}^B$ and $\vec{\phi}^A$, and $\vec{\tilde{f}}$ interpolates between $\vec{\phi}^{B'}$ and $\vec{\phi}^A$. Straightforward analogs of Eqs. (14), (16), and (17) can be written down. The net free-passage field excursion is given by Eq. (10). A crude self-consistency condition for a successful kick is therefore

$$\frac{1}{1-u^2} \gtrsim 1 + \frac{\alpha^{-1}}{|(\vec{\phi}^B + \vec{\phi}^{B'})/2 - \vec{\phi}^A|} \frac{1}{\mu^2} \left| \frac{\partial V}{\partial \vec{\phi}} \right|, \tag{20}$$

where the derivative is evaluated at $\vec{\phi} = \vec{\phi}^B + \vec{\phi}^{B'} - \vec{\phi}^A$, and μ^{-1} is the rest-frame thickness of the thicker wall. The same caveat about a vanishing potential gradient at the excursion point for the single field applies here as well.

To close this section, let us state the *transition condition* for the creation of a bubble inhabiting a new (i.e. neither parent nor original bubble) vacuum via a collision: the collision energy must be high enough to satisfy Eq. (20), and the free-passage excursion must take the field to within the basin of attraction of a new vacuum.

IV. NUMERICAL SOLUTIONS

In this section, we display a number of 1 + 1 and 3 + 1 dimensional numerical solutions to test our analytic results so far, namely, the free-passage kick Eq. (7), and the minimum energy condition Eq. (18). We adopt the following potential (Fig. 5):

$$V_3(\phi) = \frac{\lambda}{4}\phi^2(\phi - \phi_0)^2(\phi + \phi_0\eta)^2 + \epsilon\lambda\phi_0^5(\phi - \phi_0), \tag{21}$$

where we label the subscript 3 to signify that there are three minima associated with this model. There are four free parameters in this model: λ and ϕ_0 represent the overall scaling of the height and breath of the potential, ϵ breaks

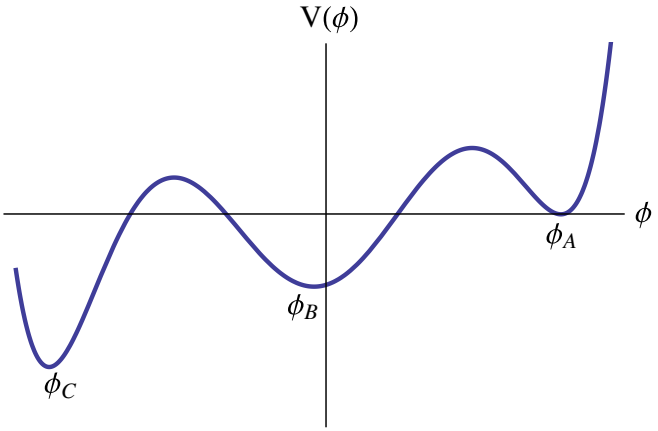

FIG. 5 (color online). The potential Eq. (21) with three minima at ϕ_A, ϕ_B, and ϕ_C. For the 3 + 1 simulations, we nucleate two bubbles of ϕ_B from a sea of ϕ_A at the distance $d = 2\gamma R_0$, where R_0 is the initial bubble radius and γ is the Lorentz factor at collision.

[3]In this case, if the different minima are degenerate, the outgoing pair of objects are then true solitons, and Eq. (18) can be replaced by $1/(1-u^2) \gtrsim m_{\rm out}^2/m_{\rm in}^2$, where $m_{\rm out}$ and $m_{\rm in}$ are the rest mass (or tension) of the outgoing and incoming solitons, i.e. $m = \int d\phi\sqrt{2V}$ with the limits of integration ranging over the appropriate vacua (V being set to zero at ϕ^B and ϕ^A). Energy conservation implies $m_{\rm out}^2/m_{\rm in}^2 = (1-v^2)/(1-u^2)$, where v is the outgoing velocity and u is the incoming one. Demanding $v \leq 1$ yields the inequality. Allowing for radiation losses strengthens it [20].

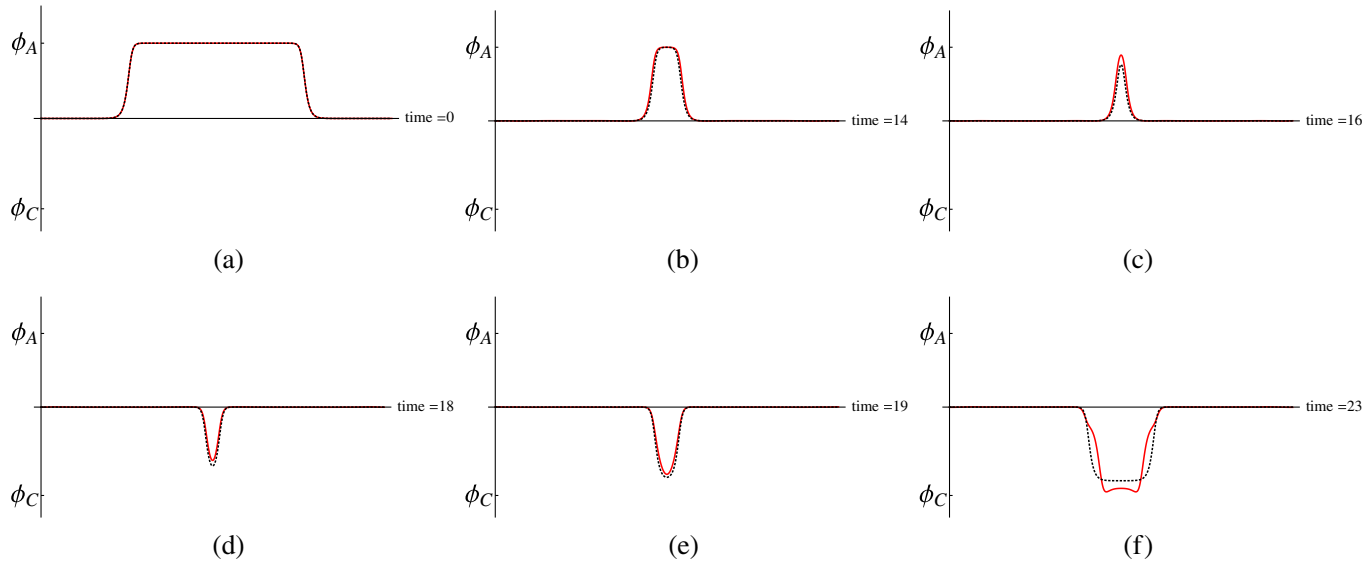

FIG. 6 (color online). These are snapshots of the 1 + 1 dimensional numerical solution to the collision of a soliton and an antisoliton, interpolating between ϕ_B and ϕ_A, as in Fig. 5. They are time ordered from (a)–(f). The red line shows the numerical solution. The dotted black line shows the free passage or linear superposition prediction Eq. (5). Here, the minimum energy condition Eq. (18) is satisfied: the threshold for the potential chosen is $\gamma_{\text{crit}} \approx 1.7$, and the γ used in the simulation is 2.3.

the degeneracy of our minima and provides the pressure that accelerates the bubble walls, and η breaks the symmetry of the potential (making the minima *unevenly* spaced and the barrier heights *unequal*). This is a modification of the canonical 3-minima model of EGHL which can be recovered by setting $\eta = 1$. Here, we adopt $\eta = 1.15$. We have neglected an additive constant to the potential, since we are working in the Minkowski limit.

Let us start with results of the 1 + 1 dimensional simulations, for which ϵ is set to zero. Here, we collide solitons that interpolate between the appropriate minima. The results are shown in Fig. 6 for a collision that meets the minimum energy condition. We can see that the free-passage approximation works very well, except in the very last snapshot. This is after the free-passage kick has been successfully realized, the field in the collision region is taken to a point just shy of the new vacuum ϕ_C. More precisely, the free-passage kick takes the field to $-\phi_0$, whereas ϕ_C is actually at $-\eta\phi_0$. The field subsequently rolls down the potential to reach ϕ_C—this subsequent evolution is not well described by free passage, as expected.

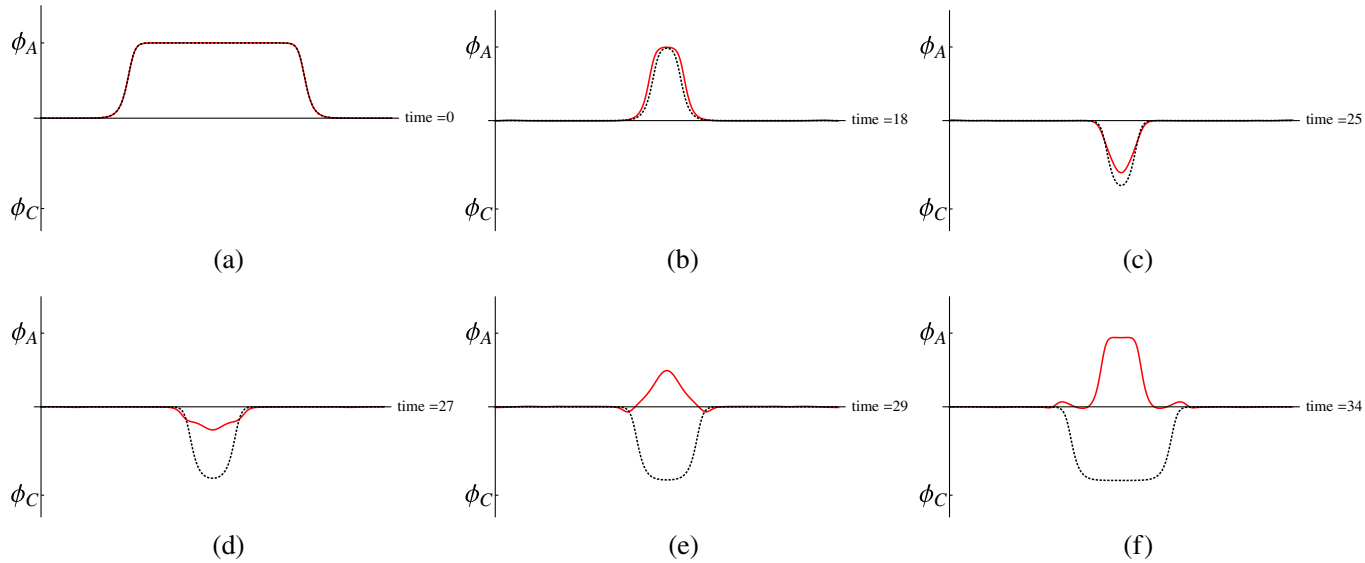

FIG. 7 (color online). Analog of Fig. 6 except that the γ used is 1.4, and therefore the free-passage kick fails, i.e. the field retreats back to ϕ_A eventually.

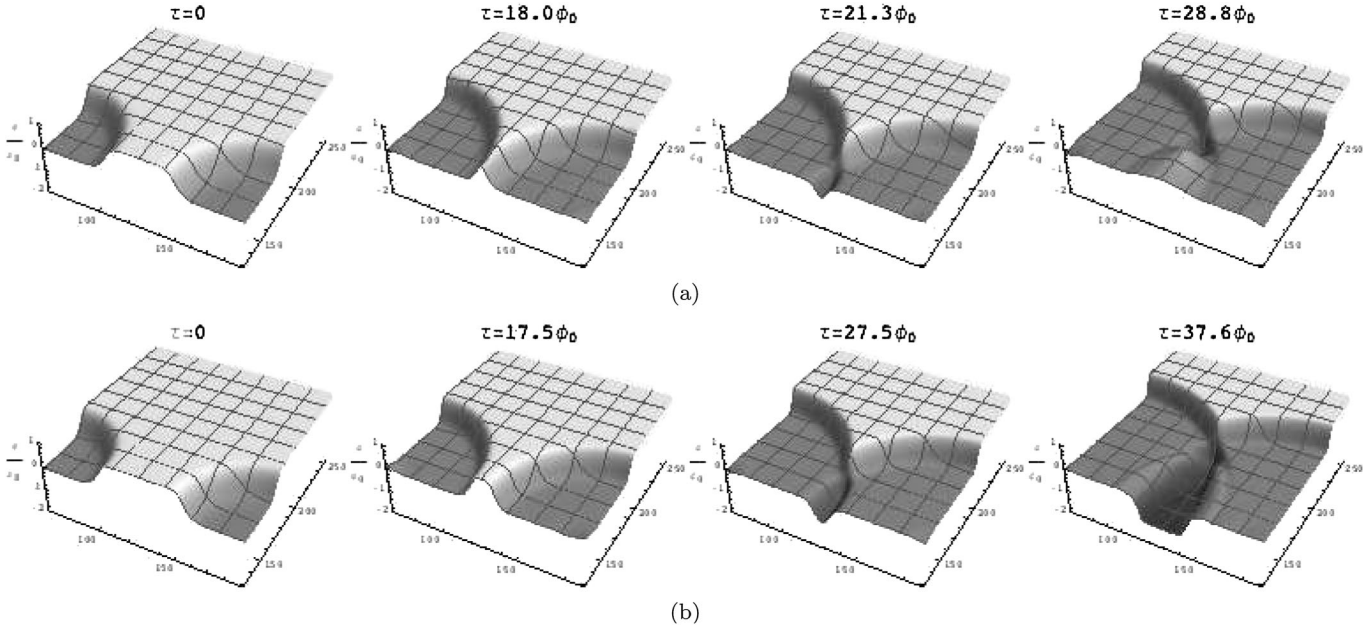

FIG. 8. The top (bottom) panels show the time evolution of two bubbles whose centers are separated by $3.0R_0$ ($3.4R_0$) so that the bubbles achieve $\gamma = 1.5$ ($\gamma = 1.7$) just before collision. Each diagram shows a 2D slice of the field values at equal time. This uses model (21) with $\eta = 1.15$.

An analogous set of snapshots for a subcritical collision is shown in Fig. 7. Here, the collision energy is not enough for the free-passage kick to succeed. Note however that the field does make a brief excursion in the direction of ϕ_C, but quickly retreats, resulting eventually in an outgoing pair of solitons that are just like the incoming ones. The free-passage approximation does not give the correct postcollision field configuration, again as expected.

For the 3 + 1 bubble (as opposed to soliton) simulations, we follow the method of EGHL for our numerics, the only difference being the potential is given by (21) and we neglect the expansion of the box for clarity as it is not essential to our work here—we have checked numerically[4] that the results do not vary much with expansion turned on in the presence of an overall vacuum energy much bigger than the energy difference between the minima. We find that the analytic arguments and 1 + 1 soliton simulations are replicated very well in the 3 + 1 dimensional simulations. The 3 + 1 simulations are crucial in confirming that there are no gross instabilities that might be missed in the 1 + 1 simulations.

We nucleate two bubbles at zero wall velocity and allow the pressure difference ($\epsilon = 1/30$) to accelerate the walls to the desired collisional γ determined by the initial separation distance d. Figures 8(a) and 8(b) show the time lapse of the results of two simulations with $\gamma = 1.5$ and $\gamma = 1.7$, with a critical $\gamma_{\rm crit} \approx 1.6$ (slightly different from the value in 1 + 1 because of the difference in ϵ). Comparing this to the theoretical expectation Eq. (18) fixes $\alpha^{-1} \approx 5.5$.

In the first simulation, we can clearly see the field attempts to execute the free-passage excursion, but due to the low collision velocity, the field does not fully transition and retreats back into the middle vacuum ϕ_B. This final behavior is unlike the soliton case, where the field retreats all the way back to ϕ_A—the difference arises because the soliton simulations have degenerate vacua, whereas ϕ_A has the highest vacuum energy in the bubble simulations. In the second simulation, the bubbles are nucleated at $d = 3.4R_0$ resulting in a $\gamma = 1.7$ at the time of collision. In this case, there is sufficient kinetic energy in the fields during the collision to ensure a transition to the lowest minimum.

V. PRODUCTION OF MULTIPLE WALLS/ SOLITONS

Suppose that in the course of the $\delta\phi$ excursion, the field passes over more than one minima (and hence more than one barrier, see Fig. 9), then given a sufficiently energetic collision, multiple barriers can be overcome and the end result is the production of multiple solitons each moving at a different velocity. Much of the discussion in the previous sections applies: the field is in free passage in the initial moments after the collision, and as the approximation breaks down, begins to feel the potential and evolve accordingly. However, the field now traverses over more than one barrier, and if the energy of the collision is high enough such that the field ends up transitioning over more than one barrier, then the free-passage ''wall'' may split into two (or more) solitons in the aftermath.

[4]We will be happy to provide the simulation results if the reader is interested.

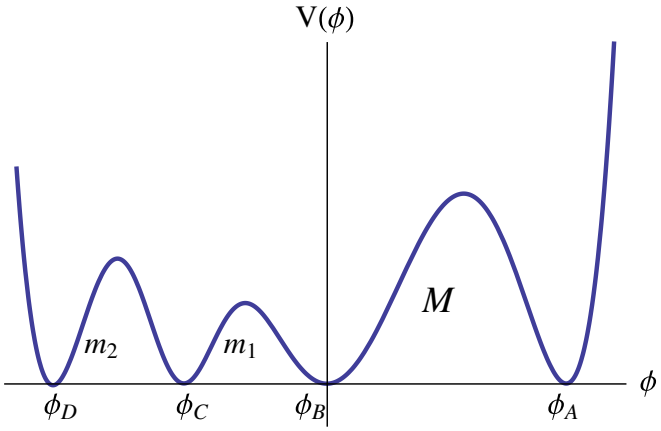

FIG. 9 (color online). A potential with four minima at ϕ_A, ϕ_B, ϕ_C, and ϕ_D. Here, M, m_1, and m_2 label the rest mass of the corresponding solitons.

Nevertheless, this does not mean that these solitons will be long lived: the splitting of the free-passage wall into two or more solitons must obey both energy *and* momentum conservation, and hence may result in the soliton with field values farthest away from the original soliton to move backward toward its mirror counterpart and annihilate each other. In the case of the solitons splitting into two, this effect can be understood by considering the solitons as massive particles and the splitting as the decay of a massive particle (the original free-passage soliton) into two less massive particles. This is then simply a kinetic problem which we can solve as follows.

Consider a potential (Fig. 9) where the incoming soliton rest mass is M and the two outgoing solitons have rest masses m_1 and m_2. According to the free-passage approximation, the incoming soliton passes through the potential barriers maintaining its field profile and velocity. Since the field now traverses a different part of the potential, this profile is no longer a solitonic solution, thus its effective rest mass is in principle undefined. To make progress, we assume that this ''soliton'' instantaneously[5] decays in the *center of mass* frame (denoted by primes) of the soliton with its incoming 4-momentum

$$P^\mu = (M, 0, 0, 0). \tag{22}$$

Meanwhile, the two outgoing solitons possess the following 4-momenta:

$$\begin{aligned} P_1^\mu &= (\gamma_1' m_1, \gamma_1' m_1 u_1', 0, 0), \\ P_2^\mu &= (\gamma_2' m_2, \gamma_2' m_2 u_2', 0, 0). \end{aligned} \tag{23}$$

Conservation of energy and momentum $P^\mu = P_1^\mu + P_2^\mu$ then allows us to solve for u_1' and u_2', which we can then transform back into the *center of collision* frame.[6] Assuming then the first soliton m_1 is formed with velocity moving away (defined to be positive) from the center of collision frame, then the second soliton has the following velocity:

$$u_2 = \frac{u_2' + u}{1 + u_2' u} \tag{24}$$

which must be >0 for the second soliton-antisoliton pair (mass m_2) not to self-annihilate.

To be specific, consider the following modification to our toy potential Eq. (21):

$$V_4(\phi) = V_3(\phi) - \delta \exp\left(-\frac{(\phi - \phi_a)^2}{b^2}\right), \tag{25}$$

where ϕ_a defines the location of an additional metastable minimum, and b^2 defines the width of that minimum. Although δ looks like a free parameter in this model, we fix it so that when $\epsilon = 0$ our minima are all degenerate, hence,

$$\delta = \frac{\lambda}{4}\phi_a^2(\phi_a - \phi_0)^2(\phi_a - \phi_0\eta)^2. \tag{26}$$

This potential is equivalent to the soliton potential shown in Fig. 9. For a model with $\eta = 1.15$, $\phi_a = 0.65\phi_0$, and $b^2 = 0.8\phi_0^2$, one can calculate that for $u_2 = 0$ (i.e. the critical splitting velocity) $\gamma = 2.3$. Colliding the solitons at $\gamma = 2.6$, we can use Eq. (24) to find that the second soliton will have a velocity of $u_2 \approx 0.2$ and hence a splitting will occur, a result which is numerically confirmed in Fig. 10.

As a final numerical test, we show that such splittings occur even in 3 + 1 dimensional simulations. We use the same potential (25) as in the solitonic case, except that we have added in a small linear tilt term $(1/30)\lambda(\phi - \phi_A)\phi_0^5$. Since we anticipate that a highly relativistic collision is necessary to produce multiple domain walls, we begin by nucleating two bubbles at a separation of $d = 5.2R_0$. Figure 11 shows the time evolution of these events. We can clearly see the free passage of the field during the collision, and then the creation and acceleration of two domain walls, making a double bubble.

Finally, we comment on an interesting possibility. Consider the case such that the collision γ is barely insufficient to satisfy Eq. (24). In this case, a fully formed

[5]This assumption is in keeping with the spirit of the free-passage approximation, although one can argue that the decay is a 2-step process in the following sense: the incoming solitons pass through each other in free passage, and then either gain or lose mass due to the fact that their profiles no longer traverse the original potential resulting in a change in velocities, before decaying.

[6]In this example, we have assumed that both incoming solitons have identical rest masses; hence this frame (where the incoming velocities are equal and opposite) is also the center of mass frame for the total system.

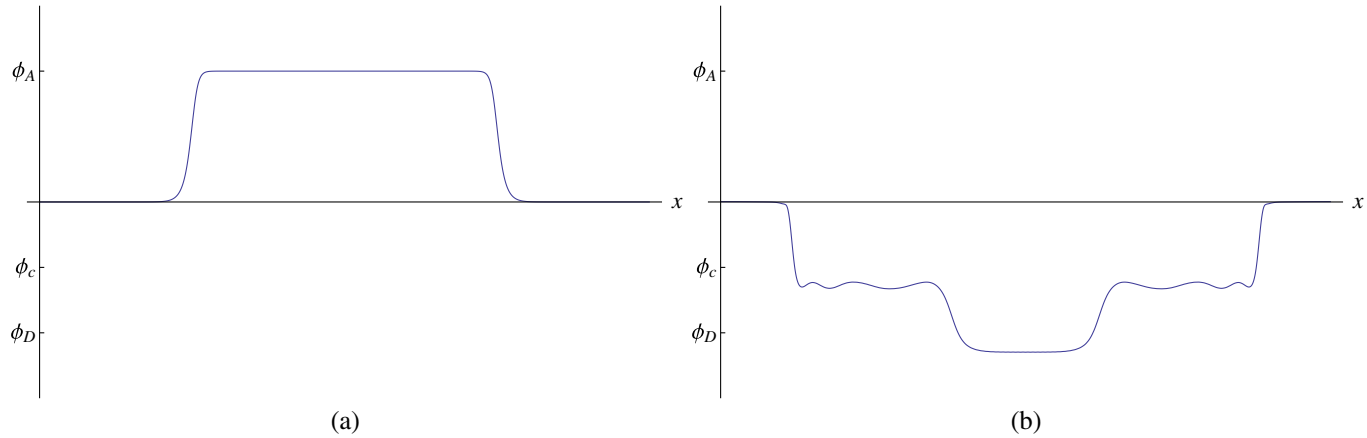

FIG. 10 (color online). The interaction of a soliton-antisoliton pair in the presence of the potential denoted in Fig. 9 and Eq. (25) with $\eta = 1.15$, $\phi_a = 0.65\phi_0$, and $b^2 = 0.8\phi_0^2$. The incoming soliton-antisoliton pair spans the barrier from ϕ_A to ϕ_B (a). Given a sufficiently energetic collision—$\gamma > 2.3$ for this potential—the field can transition to ϕ_D, forming a pair of solitons (and a pair of antisolitons) in the process (b). In general, the outgoing pair of solitons possess different velocities depending on their rest masses and the actual collision energy. For some potentials, the process can be thought of as annihilation of the two incoming solitons to form a pair of temporary free-passage solitons with the same mass, and then the decay of these solitons into two pairs of less massive solitons. Since the interaction is not completely elastic, scalar radiation visible as superimposed small perturbations is emitted.

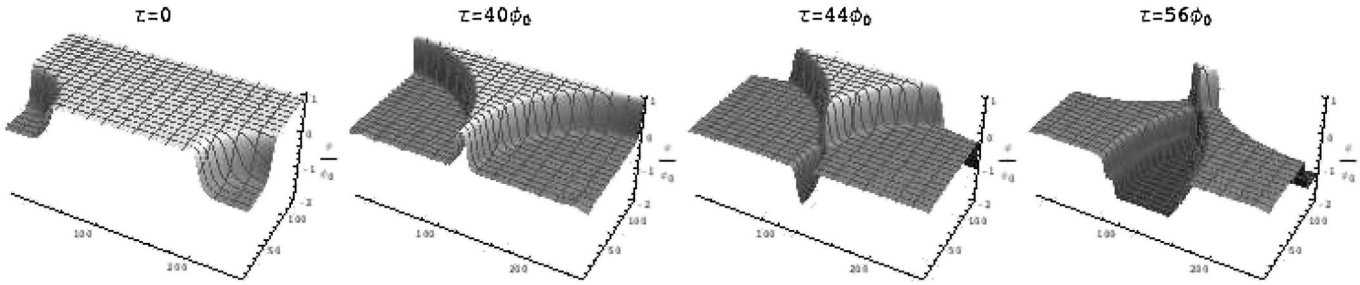

FIG. 11. The time evolution of two bubbles whose centers are separated by $5.2R_0$ so that the bubbles achieve $\gamma = 2.6$ just before collision. This uses the model (25) with $\eta = 1.15$, $\phi_a = 0.65\phi_0$, and $b^2 = 0.8\phi_0^2$. Periodic boundary conditions produce multiple images of this collision in these panels.

soliton-antisoliton pair between ϕ_C and ϕ_D is formed but self-annihilates after a while. This secondary collision can be treated as any other collision—if the right conditions are satisfied then we can form a pocket of ϕ_B vacuum, creating a ''bubble within a bubble'' scenario.

VI. DISCUSSION

To briefly summarize, we find that linear superposition of wall profiles provides a good approximation to what happens at a high-speed collision. The free passage of wall profiles implies a field excursion in the collision region that is given by Eq. (10). For this free-passage kick to be successfully realized, the collision must exceed a certain minimum energy threshold given by Eq. (18). Beyond this threshold, the size of the kick itself is independent of the collision speed, i.e. one cannot obtain arbitrarily large-field excursions by pumping up the collision energy. When the minimum energy condition is met, the free-passage kick can cause a transition into a new vacuum, if the kick takes the scalar field to within the new vacuum's basin of attraction. Interesting possibilities arise if the excursion traverses over several new vacua, and they can be understood by similar arguments (Sec. V). We have verified these statements using numerical computations of soliton collisions in $1 + 1$ and bubble collisions in $3 + 1$.

These findings have many interesting theoretical and observational implications. Let us discuss some of them.

A. Including gravity

Our simulations used a flat, nonexpanding background. To study a classical transition in the cosmological context, first we need to know the necessary modifications once we include gravitational effects.

Since the collision happens on a short time scale, the corrections from gravity will not be in the collision itself, but in the domain wall motions before and after the colli-

sion. Without gravity, it appears that arbitrarily high barriers can always be traversed via collisions, as long as the incoming boost γ is large enough. In an expanding background, however, there is a maximum boost for every collision,

$$\gamma_{\max} \sim (R_0 H_A)^{-1}, \tag{27}$$

where R_0 is the initial size of the bubble B, and H_A is the Hubble expansion rate for the parent vacuum A. Therefore, it is easy to generalize our results to an expanding background, as long as we maintain an additional condition: the critical γ to make the transition in flat space has to be smaller than $\gamma_{\max}$ in the expanding background, otherwise there will be no transition.

After the transition, there are more complications. For example, if $V_C > V_B$, the domain walls can turn around and may or may not collide with each other again, thereby sealing the vacuum C region. Also when the domain wall is heavy, $m_{BC} < |V_C - V_B|$, gravity allows it to accelerate and eventually run away from both sides. These behaviors are hard to keep track of in lattice simulations. An analytical study on these questions can be found in [22].

B. Cosmology after a collision

Many recent studies discussed the possibility of observing signals from bubble collisions in our past. Several cases are summarized in [2]. One important issue is whether slow roll inflation can be maintained after a violent disturbance like a bubble collision. The scalar field behavior we study here provides useful intuition to address such a problem.

If the field range of slow roll on the potential is super-Planckian, which is usually known as a large-field slow roll inflation, then it is quite stable against disturbances as we do not expect the vacuum separation (which determines the collision-induced kick) to be super-Planckian. A sufficiently large flat region in the potential postcollision would provide a buffer for slow roll to continue unscathed. On the other hand, if the slow roll range is smaller, then it is more delicate. One example in [2] seems to suggest that a collision always ends small-field slow roll inflation. Here we would like to argue the opposite—having small-field slow roll inflation after a collision is as plausible as having it after a Coleman–De Luccia tunneling.

We start from Fig. 7 in [2], which the authors interpreted as the collision pushing the field from slow roll directly to the end of inflation. The free passage tells us that right after the domain walls cross each other, the field ends up within a region (possibly very) near the parent vacuum (see Fig. 7 of [2]). Because of the pressure difference, such a region undergoes oscillations and recollisions as in [17]. In the figure cited above, the first two collisions are visible but the rest of them are too small to be resolved, forming an effective domain wall.[7] The pressure difference between the bubbles on the left and the right accelerates this effective domain wall to the right.

The creation of this domain wall is highly dissipative—scalar radiation is emitted from the point of initial collision and subsequent recollisions, and this scalar radiation is large enough in amplitude to disrupt the small-field inflation, causing the inflaton to topple off its delicately balanced potential and thermalize. In other words, the failure of small-field slow roll inflation appears to be a result of the disturbances of the repeated recollisions hidden in the effective domain wall.

Nevertheless, as we have shown in this paper, counter to the intuition that collisions are violent, classical transitions can be exceptionally gentle (recall the fairly homogeneous postcollision region in our 1 + 1 and 3 + 1 simulations). This gentleness might live in harmony with the delicate small-field potential. Consider a potential in Fig. 12. If we arrange that $\phi_A - \phi_B = \phi_B - \phi_C$, then by free passage, a collision between two bubbles of B naturally starts slow roll inflation in ϕ_C. One might argue that such a setup is finely tuned. Let us ask a different question: Can a Coleman–De Luccia tunneling from vacuum B start slow roll inflation in ϕ_C? The answer is yes, if we arrange the potential correctly—it is also finely tuned.

Although there seems to be an additional parameter γ involved in collisions, we remind ourselves of the following two facts.

(i) Our simulation shows that once the transition is allowed, increasing γ further has no impact on the field value right after the transition. Namely, the initial condition for starting the slow roll is not sensitive to the incoming boost.

(ii) In a multiverse we have an infinite number of collisions with different γ's, so it is naturally scanned and does not require further fine-tuning.

Therefore, all the fine-tuning is on the potential itself. We conclude that starting slow roll through collisions is not

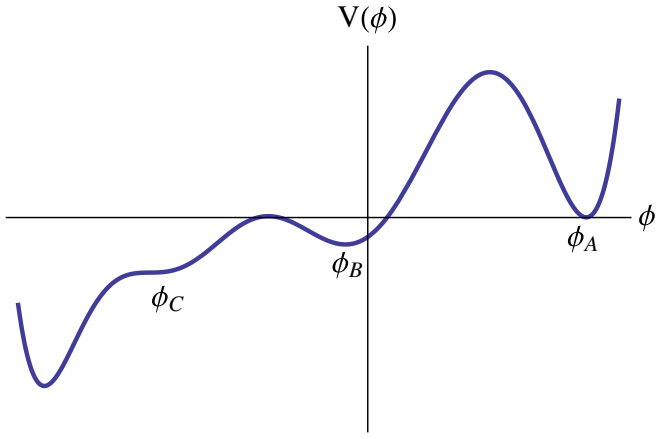

FIG. 12 (color online). A potential with vacua A, B and a small-field slow roll potential around C.

[7]We have reproduced this result in both 3 + 1 and 1 + 1.

more fine-tuned than starting it through a single tunneling.[8,9]

Let us now turn to the question of the spacetime geometry inside a collisionally formed bubble. The motivation is that we might perhaps live in it, i.e. a collision event might have constituted our beginning, our big bang. Assuming that there is slow roll inflation inside the bubble, we can approximately describe the geometry as pure de Sitter, whose general metric is given in [13]:

$$ds^2 = -\frac{dz^2}{f(z)} + f(z)dx^2 + z^2 dH_2^2, \tag{28}$$

where

$$f(z) = 1 - \frac{M}{z} + H^2 z^2. \tag{29}$$

When the domain walls are highly boosted, the conservation of the stress tensor gives us[10]

$$f_A(z_c) f_C(z_c) = [f_B(z_c)]^2, \tag{30}$$

where z_c is the collision radius of the two-dimensional hyperbolic section H_2. The A, B, C labels follow the labeling of vacua in the rest of this paper. Neglecting radiation loss (which seems to be a good approximation from our simulations), $M = 0$ in both f_A and f_B. As arranged in the potential $V_A > V_B > V_C$, M in f_C is also small and the M/z term soon becomes unimportant. The metric in region C is thus approximately

$$ds^2 = -\frac{dz^2}{1 + H_C^2 z^2} + (1 + H_C^2 z^2)dx^2 + z^2 dH_2^2. \tag{31}$$

When there is slow roll inflation in region C, this will not be the proper slicing to describe the Universe. Region C is the forward light cone of an H_2 with radius z_c. Following the usual prescription—in the case of a single bubble—for deriving an open de Sitter slicing covering the future light cone of a point in the global de Sitter space, we can similarly derive the "open" slicing of the universe in region C:

$$ds^2 = -dt^2 + \frac{\sinh^2 H_C t}{H_C^2} d\xi^2 + \left(z_c \cosh H_C t + \frac{\sinh H_C t}{H_C} \sqrt{1 + H_C^2 z_c^2} \cosh\xi \right)^2 dH_2^2. \tag{32}$$

We can see that the metric preserves only the symmetry of H_2, and is both anisotropic and inhomogeneous.[11] The interesting trait is that both its anisotropy and inhomogeneity are correlated with its negative spatial curvature. Since the universe is roughly isotropic and homogenous to 1 part to 10^5 [24], if we are to live in such a bubble, there must exist a sufficient amount of inflation in this new universe after its birth through a collision [23]. While the possibility of statistical anisotropy has been discussed, at least at the level of the initial perturbations [25], our model predicts an interesting novel anisotropy in the form of an anisotropic spatial curvature, i.e. there exist two different curvature scales in different directions, an intriguing possibility we plan to explore in future work. Note that an anisotropic curvature shifts the Doppler peaks in the microwave background on all angular scales, making the effect easier to observe than most other large scale anomalies, as recently emphasized by [26,27] in the context of other models.

C. Additional ingredients to the field dynamics

There are several possible complications to the field dynamics beyond what we have discussed. First of all, there can be derivative interactions. Our analysis should hold as long as the collision process does not probe energy scales above the cutoff for these derivative interactions, say Λ. This means the boosted thickness of our bubble walls $1/(\gamma\mu)$, where $1/\mu$ is the rest-frame thickness, must be larger than $1/\Lambda$. This implies an *upper limit* to the collision speed that we can consider $\gamma \lesssim \Lambda/\mu$. When derivative interactions are important, linear superposition such as we have used in Eq. (5) no longer works.

Another possibility is that the field metric (in the multifield case) is nontrivial, and therefore the excursion trajectory is modified. A third possibility is that some other field is coupled to our bubble scalar field, and the coupling is such that this other field becomes massless in the course of an excursion. Massless particles get produced,[12] and could significantly modify the excursion trajectory. We plan to investigate these intriguing possibilities in the future.

D. Scanning of the landscape

The collision-induced excursion offers a new mechanism for scanning a landscape of many vacua. Our results here touch on two aspects of this scanning. One is that even very high barriers can be overcome by a collision as long as the collision is relativistic enough (but subject to constraints from expansion, and from derivative interactions).

[8]These fine-tunings are only necessary in small-field inflation models. In large-field models it will be equally generic to start inflation through either tunneling or collision.

[9]It might be possible to make small-field inflation models so sensitive that they magnify the weak dependence on the incoming boost γ. Such a scenario requires a probability distribution of γ and is beyond the scope of this paper.

[10]This is exactly true for massless (null) domain walls [12], and approximately true for light or highly boosted domain walls.

[11]A similar result was found in [23], but their metric, Eq. (24), is only a special case of ours with $H_C = 0$. Our metric supports a slow roll inflating era that is essential to develop standard cosmology.

[12]In [28] it is treated as a direct generalization of preheating, but we remain conservative about their results.

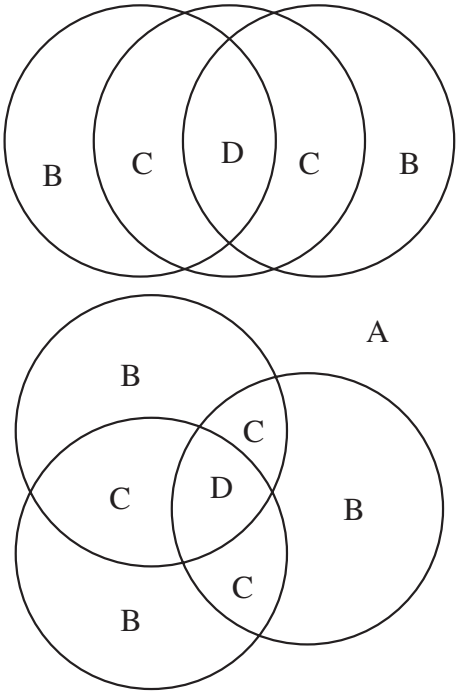

FIG. 13. A spacelike slice through multiple, overlapping collisions. Following the vector sum rule, we have $\vec{\phi}_C = 2\vec{\phi}_B - \vec{\phi}_A$, and $\vec{\phi}_D = 3\vec{\phi}_B - 2\vec{\phi}_A$.

It could well be that certain vacua surrounded by high barriers are more likely to be populated by collisions rather than direct tunneling. A second important feature of this scanning is that it is bounded—the collision-induced excursion does not become arbitrarily large by raising the collision speed. Rather, it is controlled by a simple vector sum rule (Fig. 4), which tells us that the excursion can only be as large as the field difference between the parent and bubble vacua. In theories in which tunneling between vastly separated vacua is common [29], large collision excursions are also possible. Finally, this excursion has a specific direction, and it is interesting to ask what is the typical basin of attraction there. In [30] is it suggested that due to the universal dilatonic runaway direction in string theory inspired models, classical transition can lead to decompactification of extra dimensions.

E. Multiple collisions

The free-passage approximation and the resulting vector sum rule in Sec. II are simple facts of the field dynamics. It applies to any solitonic objects interpolating between local minima. We can arrange a potential in which a collision is followed by further collisions, leading to a nested set of classical transitions. A spacetime structure with multiple, overlapping collisions follows simply from the vector sum rule, as shown in Fig. 13.

A particularly intriguing version of this occurs when a bubble is nucleated in the presence of a compact dimension [31]. The bubble grows, wraps around the compact dimension, and eventually collides with itself. A new vacuum opens up between the outgoing pair of walls. These walls eventually collide after traveling through the compact dimension. Further transitions and collisions follow, as far as the potential allows. This provides a novel way to realize an old idea by Abbott [32], by classical transitions rather than tunneling.

In the context of a scalar field, such a cascade of classical transitions seems to rely on the existence of roughly evenly spaced vacua in the potential landscape. Interestingly, in [33] it is shown that in a model with multiple vacua constructed from extra dimensions and fluxes, a classical transition is the most natural result, as shown in Fig. 14. In these models, the multiple classical transition structure in Fig. 13 should be taken seriously. A similar but simpler structure was studied in [34] and suggested the possibility of a conformal field theory description for an eternal inflating spacetime.

ACKNOWLEDGMENTS

We would like to thank Richard Easther, Brian Greene, Matt Johnson, Tommy Levi, and especially Matt Kleban, Alberto Nicolis, and Erick Weinberg for many useful discussions. This work is supported in part by the DOE No. DE-FG02-92-ER40699, and by the NASA Astrophysics Theory Program No. 09-ATP09-0049. L. H. thanks members of the CCPP at NYU and the IAS at Princeton for their hospitality. E. A. L. thanks Kenyon College, where some of this work was done, for hospitality and acknowledge the support of a Foundational Question

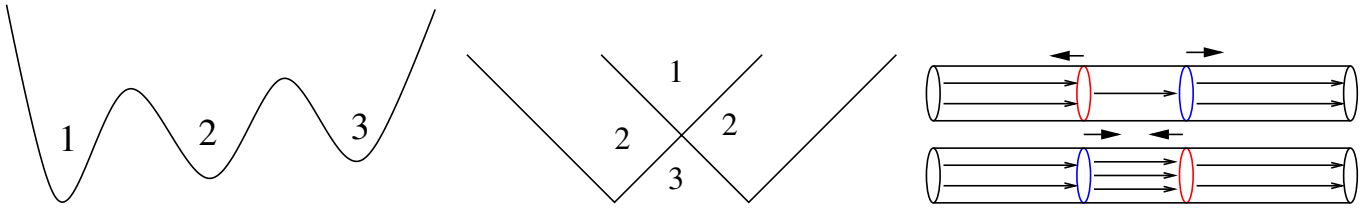

FIG. 14 (color online). A classical transition (middle panel) can occur when the positions of vacua are arranged appropriately (left panel), as demonstrated in this paper. Alternatively one can have a model like the figure on the right, where vacua 1, 2, and 3 have 1, 2, and 3 units of flux and the domain wall is the charged object which changes the flux. If the charged objects freely pass through each other, a classical transition is the most natural result of every collision.

Institute Mini-Grant. Research at the Perimeter Institute for Theoretical Physics is supported by the Government of Canada through Industry Canada and by the Province of Ontario through the Ministry of Research & Innovation.

APPENDIX: THE SINE-GORDON EXAMPLE

The sine-Gordon potential is $V = 1 - \cos\phi$ such that the equation of motion is $-\partial_t^2\phi + \partial_x^2\phi = \sin\phi$. The exact one-soliton solution is

$$\phi = 4\tan^{-1}\exp\left[\frac{x - ut}{\sqrt{1 - u^2}}\right]. \tag{A1}$$

This interpolates between $\phi = 2\pi$ to the far right and $\phi = 0$ to the far left. The exact soliton-antisoliton pair solution is

$$\phi = 4\tan^{-1}\left[\frac{1}{u}\frac{\sinh(-ut/\sqrt{1 - u^2})}{\cosh(x/\sqrt{1 - u^2})}\right]. \tag{A2}$$

This solution describes the collision of an incoming $(0/2\pi, 2\pi/0)$ pair, resulting in an outgoing $(0/-2\pi, -2\pi/0)$ pair, *irrespective* of the size of u. Note that $u = 0$ is *not* a solution—no stable static solution of more than one sine-Gordon soliton exists.

[1] R. Bousso and J. Polchinski, J. High Energy Phys. 06 (2000) 006.
[2] A. Aguirre and M. C. Johnson, arXiv:0908.4105.
[3] K. Larjo and T. S. Levi, arXiv:0910.4159.
[4] B. Freivogel, M. Kleban, A. Nicolis, and K. Sigurdson, J. Cosmol. Astropart. Phys. 08 (2009) 036.
[5] A. Aguirre, M. C. Johnson, and M. Tysanner, Phys. Rev. D **79**, 123514 (2009).
[6] S. Chang, M. Kleban, and T. S. Levi, J. Cosmol. Astropart. Phys. 04 (2009) 025.
[7] S. Chang, M. Kleban, and T. S. Levi, J. Cosmol. Astropart. Phys. 04 (2008) 034.
[8] S. G. Rubin, A. S. Sakharov, and M. Y. Khlopov, J. Exp. Theor. Phys. **92**, 921 (2001).
[9] R. Easther, E. A. Lim, and M. R. Martin, J. Cosmol. Astropart. Phys. 03 (2006) 016.
[10] J. Garriga, D. Schwartz-Perlov,A. Vilenkin, and S. Winitzki, J. Cosmol. Astropart. Phys. 01 (2006) 017.
[11] S. Coleman, Phys. Rev. D **15**, 2929 (1977).
[12] D. Langlois, K.-i. Maeda, and D. Wands, Phys. Rev. Lett. **88**, 181301 (2002).
[13] B. Freivogel, G. T. Horowitz, and S. Shenker, J. High Energy Phys. 05 (2007) 090.
[14] R. Bousso *et al.*, Phys. Rev. D **78**, 063538 (2008).
[15] A. Aguirre and M. C. Johnson, Phys. Rev. D **77**, 123536 (2008).
[16] M. Axenides, S. Komineas, L. Perivolaropoulos, and M. Floratos, Phys. Rev. D **61**, 085006 (2000).
[17] S. W. Hawking, I. G. Moss, and J. M. Stewart, Phys. Rev. D **26**, 2681 (1982).
[18] A. Kosowsky, M. S. Turner, and R. Watkins, Phys. Rev. Lett. **69**, 2026 (1992).
[19] A. Kosowsky, M. S. Turner, and R. Watkins, Phys. Rev. D **45**, 4514 (1992).
[20] R. Easther, J. T. Giblin, Jr., L. Hui, and E. A. Lim, Phys. Rev. D **80**, 123519 (2009).
[21] A. C. Scott, f. Y. F. Chu, and D. W. McLaughlin, Proc. IEEE **61**, 1443 (1973).
[22] M. C. Johnson and I.-S. Yang, arXiv:1005.3506.
[23] R. M. Wald, Phys. Rev. D **28**, 2118 (1983).
[24] E. Komatsu *et al.*, arXiv:1001.4538.
[25] L. Ackerman, S. M. Carroll, and M. B. Wise, Phys. Rev. D **75**, 083502 (2007).
[26] P. W. Graham, R. Harnik, and S. Rajendran, arXiv:1003.0236.
[27] J. J. Blanco-Pillado and M. P. Salem, J. Cosmol. Astropart. Phys. 07 (2010) 007.
[28] J. Zhang and Y.-S. Piao, arXiv:1004.2333 [Phys. Rev. D (to be published)].
[29] A. R. Brown and A. Dahlen, arXiv:1004.3994.
[30] A. Aguirre, M. C. Johnson, and M. Larfors, Phys. Rev. D **81**, 043527 (2010).
[31] A. R. Brown, Phys. Rev. Lett. **101**, 221302 (2008).
[32] L. F. Abbott, Phys. Lett. **150B**, 427 (1985).
[33] J. J. Blanco-Pillado, D. Schwartz-Perlov, and A. Vilenkin, J. Cosmol. Astropart. Phys. 12 (2009) 006.
[34] B. Freivogel and M. Kleban, J. High Energy Phys. 12 (2009) 019.